Holographic study of conventional and negative Poisson's ratio metallic foams: elasticity, yield, and micro-deformation

by

C. P. Chen
and
R. S. Lakes

J. Materials Science, 26, 5397-5402 (1991)

Abstract

This article presents an experimental study by holographic interferometry of the following material properties of conventional and negative Poisson's ratio copper foams:Young's moduli, Poisson's ratios, yield strengths, and characteristic lengths associated with inhomogeneous deformation. The Young's modulus and yield strength of the conventional copper foam were comparable to those predicted by microstructural modelling on the basis of cellular rib bending. The re-entrant copper foam exhibited a negative Poisson's ratio as indicated by the elliptic contour fringes on the specimen surface in the bending tests. Inhomogeneous, non-affine deformation was observed holographically in both foam materials.

Introduction

Conventional foams, like other ordinary materials, exhibit a positive Poisson's ratio, that is, they become smaller in cross-section when stretched and larger when compressed. Recently, the invention of negative Poisson's ratio foams was reported[1,2,3]. Foam materials based on metal and several polymers were transformed so that their cellular architecture became re-entrant, i.e. with inwardly protruding cell ribs. Foams with re-entrant structures exhibited negative Poisson's ratios as small as -0.7 as well as greater resilience than conventional foams.

Material properties of conventional and re-entrant copper foams have been determined from uniaxial compression tests using an MTS materials testing machine[3]. Engineering stress-strain graphs were extracted from load-displacement data. The Poisson's ratios of specimens in this series were determined from displacement measurements of high magnification video tapes of the tensile tests. However, other methods, which complied with ASTM standards, of measuring Poisson's ratio were tried and found unsuitable due to the inherently rough, porous surface of the foams.

The laser interferometric method has been presented in the literature for determining the displacement field on the surface of a specimen and therefore the specimen's properties. The hyperbolic contour lines on the lateral surface of a bent specimen can be viewed interferometrically and used to determine the specimen's Poisson's ratio[4]. The deformation of an object can be investigated from the fringes on a hologram film by means of double-exposure holographic interferometry[5]. It has also been concluded that the laser interferometry technique offered a very useful and reliable tool to determine the Poisson's ratio of orthotropic FRP (Fiber Reinforced Plastics) plates[6]. Holographic interferometry provides interferometric accuracy for deformation measurements of rough surfaces; this feature is of particular use for cellular solids.

As for deformation mechanisms and structure-related behavior, rotational degrees of freedom were examined in earlier articles[7,8]. The method involved inference from nonclassical size effects in the bending and torsion rigidity as determined using a micromechanics apparatus. Moreover, dispersion of standing waves and cut-off frequencies in torsional vibration were observed for the foam materials[9]. These nonclassical phenomena were attributed to the material microstructure in a structural view.

The present study applies double-exposure holographic interferometry to determine the material properties (Young's moduli, Poisson's ratios, and yield behavior) of conventional and negative Poisson's ratio foam, as well as to explore the non-affine deformation associated with movements of the microstructure. Affine deformation is locally equivalent to a superposition of a strain and a rotation.

Material and method

Bending experiments were conducted upon conventional and re-entrant copper foam specimens at room temperature. The conventional copper foam used was open cell with density 0.795 g/cm^3, solid volume fraction 0.089, and cell size 0.4 mm. The copper foam was transformed into re-entrant structure by successive applications of small increments of plastic deformation in three orthogonal directions, as described earlier[1,3]. The density of the re-entrant copper foam tested here was 2.43 g/cm^3 with a permanent volumetric compression ratio of approximately 3, and solid volume fraction 0.27. The foams were machine finished to obtain the desired surface smoothness. The dimensions of the conventional copper foam specimen was 9 mm by 15 mm in cross section and 34 mm in length; and of the re-entrant specimen, 6 mm by 6.5 mm in cross section and 26 mm in length.

The lower end of each specimen was cemented firmly on a precision tilt/rotation base (Newport Corporation). The upper specimen end was cemented to an aluminum cantilever beam upon which weights were placed to achieve bending. The aluminum beam was sufficiently long so that it was possible to neglect the axial compression caused by the weight in comparison with strain due to bending. The specimen was thus deformed by a nearly pure bending moment. The fringe pattern was centred to facilitate the determination of Poisson's ratio from the hyperbolic or elliptical fringe pattern. This was done by tilting and rotating the base between the holographic exposures.

The specimens and the holographic components were installed on a research grade damped table top supported upon four pneumatic isolation mounts (Newport Corporation). The lab ventilation was shut off during the experiments to eliminate air currents and noise. A beam from a 15 milliwatt helium-neon laser was divided by a beamsplitter into an object beam and a reference beam. The following configuration was used for zero-order fringe analysis described

below. Image plane transmission holograms were made of the tensile side of the bent specimen via a unity magnification configuration using a six element coated f/1.2 lens system of focal length 150 mm. For the purpose of simplifying the calculation, the reference and reconstruction beams were collimated. Moreover the object illumination beam was collimated and directed perpendicular to the specimen surface by a plate beamsplitter, as shown in Fig. 1. Each exposure was about three seconds, achieved using a digitally controlled shutter. Further image plane holograms were made, without specimen tilt, for Haidinger fringe analysis using an f/0.7 lens system consisting of two f/1.4 camera lenses of 50 mm focal length and seven elements each, placed front to front. The rationale was to improve the quality of the Haidinger fringes and achieve a wider exit cone of projected rays. Agfa 8E75 holographic film was used, was developed in Kodak D19 and bleached in ammonium dichromate bleach to increase the brightness. The images were viewed in laser light of 633 nm wavelength, the same as was used for making the holograms.

Bending test: zero-order fringe interpretation

The zero-order fringe method (ZF)[5] was used to obtain the specimen's Young's modulus and Poisson's ratio, for study of residual strain due to yielding, and for study of inhomogeneous deformation. The relation between the displacement vector u and the fringe order n at a point P on the illuminated surface of the specimen is given by

$$n\lambda = u\ (k - h) \qquad (1)$$

in which λ is the wavelength of the light, k is the unit vector from the object to the observer's eye, and h is the unit vector from the light source to the object. The fringe order n represents the total displacement vector of points on the specimen surface. The center of the fringe pattern was the location where the lateral movement was zero.

Eq. 1 is simplified if the illumination and observation directions are arranged to be collinear in the z direction perpendicular to the specimen surface. This was achieved in the experiment via the configuration shown in Fig. 1. Collimated object illumination was used so that the illumination direction did not vary with position. Under these conditions, Eq. 1 becomes

$$\frac{n\lambda}{2} = u_z \qquad (2)$$

in which u_z is the displacement of point P in the z direction (out-of-plane, along the line of sight) and can be obtained from the fringe order n.

The macroscopic strain ε on the lateral surface of the beam as a result of bending deformation was given as[10]

$$\varepsilon = \frac{2y}{L^2}\ u_z \qquad (3)$$

in which y is the distance from the point P at which the strain is measured to the neutral surface of the beam or one half of the beam thickness for a rectangular cross section specimen, and L is the distance between point P and the center of the fringe pattern. The Young's modulus E of the specimen is defined as $E=\sigma/\varepsilon$, or, from the elementary theory of bending in classical elasticity,

$$E = \frac{M L^2}{2 u_z I} \qquad (4)$$

in which M is the bending moment, and I is the moment of inertia of the cross section area of the specimen.

The fringe pattern on the specimen's surface can also be used for determining the specimen's Poisson's ratio ν. The contour lines of constant u_z was given, based on classical elasticity, as[4]

$$z^2 - \nu y^2 = \text{constant} \qquad (5)$$

The contour lines of the lateral displacement field of the specimen, or the observed interference fringes, are therefore hyperbolae for specimens of positive Poisson's ratio and ellipses for those of negative Poisson's ratio, respectively. The Poisson's ratio ν was also given as

$$\nu = \tan^2\alpha \qquad (6)$$

in which 2α is the angle between the asymptotes of the hyperbolae as given by Equation (5).

Holographic exposures were made of bent specimens at progressively larger loads, with the aim of exploring the onset of inhomogeneous deformation associated with the microstructure as manifested by irregularity and breakup of the fringe pattern.

This holographic interferometry and data reduction scheme was first verified by tests upon a PMMA (Polymethyl Methacrylate or Plexiglas®) specimen, which has independently determined properties[11]. The PMMA specimen was 9 mm by 12.5 mm in cross section and 88 mm in length. White paint was sprayed on the illuminated surface of the PMMA specimen for the purpose of maximizing the diffuse light reflection.

Yielding test

A holographic exposure was made of the specimen without any bending load. The bending load was then applied for 30 seconds and removed. The second exposure was taken 30 seconds later after the load was removed. If yielding has occurred, there will be some residual strain, resulting in fringes in the hologram. Based on a series of holograms being taken with increasing loads, the yield strength of the specimen was determined.

Study of non-affine deformation

Non-affine deformation was studied both by the zero order fringe method and by the Haidinger fringe method. In the zero-order fringe method, inhomogeneous deformation of the non-affine type manifests itself as a bumpiness or breakup of the fringes covering the specimen. The optical system in Fig. 1, used for zero-order fringe analysis, is sensitive to out-of-plane deformation, perpendicular to the specimen surface, so that is also the sensitivity direction for non-affine deformation. The Haidinger fringe method discloses the vector displacement of an individual object point[5,12]. The x component of in-plane displacement U_x is given by

$$U_x = \lambda / \xi_x \qquad (7)$$

in which λ is the wavelength of light and ξ_x is the x component of angular spacing, in radians, of the projected fringes; similarly for the y direction. In this method, the corresponding image point was illuminated by a concentrated laser beam, focused to a spot size less than 0.2 mm in diameter, in the direction of the original reference beam. Diffracted light formed a pattern of fringes which was projected upon a ground glass, as shown in Fig. 2. The light beam was slowly scanned across the specimen and inferred displacements of nearby points were compared to determine the micro-strain. In this experiment, non-affine deformation manifests itself as micro-strain differing from macroscopic strain.

Microstructural analysis

The mechanical properties of foams can be related to the properties of the cell material and geometry[13]. For conventional open cell foam[13],

$$\frac{E}{E_s} = \left(\frac{\rho}{\rho_s}\right)^2 \qquad (8)$$

on the basis of simple bending of the cell ribs, in which E and ρ are the Young's modulus and mass density of the foam, and E_s and ρ_s are the Young's modulus and mass density of the solid of which the foam was made.

Cellular materials can collapse. Plastic collapse occurs when the moment exerted on the cell ribs exceeds the fully plastic moment, creating plastic hinges. The plastic collapse stress, or the yielding strength of the foams was given as[13]

$$\frac{\sigma_y}{\sigma_{ys}} = 0.3 \left(\frac{\rho}{\rho_s}\right)^{3/2} \qquad (9)$$

in which σ_y and σ_{ys} are the yield strength of the foam, and the solid of which the foam was made of, respectively.

The properties of solid copper were taken as E_s = 119,000 MPa, ρ_s = 8.93 g/cm^3, and σ_{ys} = 62 MPa[13,14]. Substitution of the foam densities mentioned in the previous section in

Equations (8) and (9) yielded theoretical values of the foam properties. The Young's modulus E, and yield strength σ_y of the conventional copper foam were predicted to be 943 MPa, and 0.49 MPa, respectively. The prediction of the properties of the re-entrant foams was not attempted since Equations (8) and (9) are only applicable to conventional foams with straight cell ribs.

Results and discussion

A typical fringe pattern of the PMMA specimen is shown in Fig. 3. Analysis of the fringe orders at different locations via Equation (3) disclosed that uniform strain was obtained on the specimen surface in bending. The Young's modulus E was obtained to be approximately 2.6 GPa, and the Poisson's ratio ν was obtained to be 0.33 from Equations (4), and (6), respectively. The experimental values of E and ν were in good agreement with those independently determined[11]. The fringes of the hyperbolic contour lines remained of high contrast up to high fringe density corresponding to a bending strain 0.00084. Consequently the PMMA did not exhibit any inhomogeneous deformation, as expected in view of classical elasticity or viscoelasticity.

Fig. 4 shows the fringe pattern of the conventional copper foam. These fringes represent hyperbolic contour lines which show the anticlastic curvature of a positive Poisson's ratio material, just as the case with PMMA. The measured asymptotic angle α was substituted into Equation (6) to obtain the Poisson's ratio ν of the conventional copper foam as 0.25. Conventional foams usually have Poisson's ratios closer to 0.3, but there is considerable variation[13]; indeed, a different density copper foam[3] had a Poisson's ratio of 0.4. The Young's modulus E was found to be approximately 900 MPa, at a macroscopic stress 0.15 MPa and strain 0.00017. The experimental value of E agreed reasonably well with 943 MPa predicted from Equation (8) in the previous section. Fig.5 shows the residual strain vs the applied strain for conventional copper foam obtained by the yielding tests. The yield strength σ_y of the conventional copper foam was found to be approximately 0.42 MPa. The yield strength predicted by Equation (9) was 0.49 MPa. The agreement is considered satisfactory in view of the fact that a book value for the (0.2%) yield strength of solid copper was used in the calculation. The yield strain of the foam was 0.00047.

The fringe pattern for the foams became less clear as the load level increased. On close examination, the fringes were seen to become progressively more bumpy with increase in load. The clarity of the fringe pattern was represented quantitatively by d/D, in which d is the width of the pattern of bumps of two neighboring fringes and D is the overall fringe width, and is shown in Fig. 6, with an estimated 10% error range. As progressively higher loads were applied to conventional foam, fringes began to become bumpy at strains of 0.000062 and were

very broken up at strains of ε=0.00032 to 0.00037. Complete fringe breakup occurred at strains below the yield strain and so cannot be a result of yielding.

Fig.7 shows the fringe pattern of the re-entrant copper foam. The fringe pattern of elliptic contour lines indicated that the Poisson's ratio of the re-entrant copper foam was negative. The Young's modulus E was obtained to be approximately 480 MPa, at a macroscopic stress of 0.032 MPa and strain 0.00067. This result is consistent with the fact that theYoung's modulus of the foam materials has previously been found to be reduced by re-entrant transformation[3]. The Poisson's ratio ν for this specimen was obtained to be -0.11; lower density copper foam[3] in simple compression had a Poisson's ratio of -0.4. Figure 6 shows the residual strain as it depends on the applied strain of the re-entrant copper foam. The yield strength was determined to be 0.35 MPa by the yielding tests, and the yield strain was 0.00072.

The predictions of the properties of the conventional copper foams by Equations (8) and (9) on the basis of solid volume fraction were obtained with some structural assumptions. However, the yield strength σ_y of the foam materials can also be obtained by substituting Equation (8) into Equation (9) to obtain $\sigma_y/\sigma_{ys}=0.3(E/E_s)^{3/4}$ with the solid volume fraction eliminated. With E=480 MPa substituted, the yield strength σ_y for re-entrant copper foam was calculated from this expression to be 0.3 MPa. This was comparable to 0.35 MPa obtained by the yielding tests on the re-entrant copper foam even though Equations (8) and (9) individually do not apply to re-entrant foam.

Fringes in the re-entrant foam began to get bumpy at a macroscopic strain of 0.00021 and were totally broken up at a strain of from 0.00063 to 0.001. In this case the strain for total fringe breakup and the strain for yield were comparable. Nevertheless, the onset of fringe bumpiness or breakup occurred well below the yield point, as shown in Fig. 6.

The loss of fringe clarity in the foams at higher loads was not a simple loss of contrast associated with a hologram of a field of homogeneous strain and rotation[5] viewed through a large pupil; there was no such effect in the PMMA which is a homogeneous material. The fringes in the foam became noticeably bumpy before they broke up. The effect is attributed to inhomogeneous deformation associated with the microstructure, specifically a non-affine deformation which cannot be described as a superposition of homogeneous strain and rotation. Quantitative measures of such inhomogeneous deformation may be defined as follows: the ratio Γ of micro-strain to macro-strain ε_{macro}, $\Gamma = (\delta/d_{cell})/\varepsilon_{macro}$; and a micro-deformation characteristic length $\ell_m = \delta/\varepsilon_{macro}$ in which δ is the inhomogeneous micro-deformation and d_{cell} is the cell size. In the present zero-order fringe experiments the fringes become totally fragmented when the micro-deformation over one cell is one fringe or half a wavelength of red light, so δ = 0.3 μm. The cell size is 0.4 mm for conventional foam and $0.4mm/(3)^{1/3}$ for re-entrant foam.

Consequently, for conventional foam, $\Gamma_{avg,} = 2.1$, $\lambda_m = 0.86$mm; for re-entrant foam, $\Gamma_{avg,} = 1.3$, $\lambda_m = 0.38$mm. The non-affine motion disclosed by these experiments is an average value perpendicular to the specimen surface.

The Haidinger fringe experiments disclosed largely in-plane motions along the specimen long axis. The calculated micro-strains ranged from -0.004 to 0.004 for a macro-strain of 0.00079, for the conventional copper foam; and from -0.0013 to 0.0028 at a macro-strain of 0.0008 for the re-entrant copper foam. The ratios of the maximum micro-strain to the macro-strain were thus determined to be $\Gamma_{max\|} = 5.1$, and 3.5 for the conventional copper foam, and the re-entrant copper foam respectively. The non-affine motion disclosed by these experiments is a maximum value parallel to the specimen surface.

The inhomogeneous, non-affine micro-deformation observed in the foams has several interesting implications. For example, such deformation, as well as a local rotation of points has been incorporated into generalized continuum theories known as 'microstructure'[16] or 'micromorphic'[17] elasticity. In comparison, Cosserat solids[7,8] admit rotations and translations, and classically elastic solids admit only translation of points. A material obeying generalized continuum theory may exhibit stress concentration factors which are less or greater than classical values, depending on the values of the extra material constants prescribed by the theory[18]. The micro-deformation and local rotation degrees of freedom are therefore intimately connected with the toughness of these materials. The micro-deformation is, moreover, associated with unusual acoustic behavior, both in the context of generalized continuum mechanics[16], and experimental dynamic measurements[9]. However, we do not at this time have the ability to predict or control the acoustic behavior based on non-affine deformation kinematics. Microstructural degrees of freedom are also associated with the Poisson's ratio: negative Poisson's ratios may result from non-affine deformation kinematics or from rotational degrees of freedom combined with prestrain[19]. Rotational freedom is doubtless present in view of the bending moments transmitted through the cell ribs[2], however that alone need not give rise to a negative Poisson's ratio[19]. The present study has demonstrated the presence of non-affine deformation in both the conventional and re-entrant metal cellular solids. We remark that the measurements were made at the specimen surface, where some cells were incomplete as a result of cutting. Consequently there is the possibility that the surface is not equivalent to the bulk material. The larger non-affine effects in the conventional foam was surprising in view of qualitative observations of unfolding of cells in stretched re-entrant polymer foam, which suggested that larger effects would occur in the re-entrant material. However, it cannot be assumed that the deformation kinematics are identical in the polymeric and metallic foams; further study is anticipated to resolve this issue.

Conclusions

1. The holographic interferometry technique was found to be a useful method to determine the elastic properties of the foam materials. It was verified by using it to examine a PMMA specimen, which has independently determined properties.
2. The Young's modulus E, yield strength σ_y, and Poisson's ratio ν of the conventional and negative Poisson's ratio copper foams were determined in bending tests by the holographic interferometry. The Young's modulus of the conventional copper foam was found to be twice that of the corresponding re-entrant negative Poisson's ratio foam. The yield strength was approximately the same for the conventional and negative Poisson's ratio copper foams.
3. The Young's modulus and yield strength of the conventional copper foam were comparable to those predicted by microstructural analysis based on cellular rib bending.
4. Inhomogeneous, non-affine deformation was inferred from the bumpiness and breakup of the holographic fringes with increasing load. The effects were larger in the conventional foam.

References

1. R. S. Lakes, "Foam structures with a Negative Poisson's ratio", Science 235 (1987),1038-1040 .
2. R. S. Lakes, "Negative Poisson's ratio materials", Science 238 (1987), 551.
3. E. A. Friis, R. S. Lakes, and J. B. Park, "Negative Poisson's ratio polymeric and metallic foams", J. Materials Sci. 23 (1988)4406-4414.
4. S. P. Timoshenko and J. N. Goodier, Theory of elasticity, McGraw-Hill, 3rd edition, (1970).
5. W. Schumann and M. Dubas, Holographic interferometry, Springer-Verlag, (1979).
6. R. M. V. G. K. Rao, M. Swaminadham, and K. Rajanna, "Effect of moisture and glass contents on the Poisson's ratio of FRP plates as determined by laser interferometry", Fibre science and Technology 15 (1981) 235-242.
7. R. S. Lakes, "Size effects and micromechanics of a porous solid", J. Materials Sci. 18 (1983) 2572-2580.
8. R. S. Lakes, "Experimental microelasticity of two porous solids", Int. J. Solids, Structures, 22 (1986)55-63
9. C. P. Chen, and R. S. Lakes, "Dynamic wave dispersion and loss properties of conventional and negative Poisson's ratio polymeric cellular materials", Cellular polymers 8(1989)343-359
10. S. P. Timoshenko and J. M. Gere, Mechanics of materials, Litton Educational Publishing, Inc., (1972).
11. J. D. Ferry, Viscoelastic Properties of Polymers , J. Wiley, 2nd edition, (1970).

12. Briers, "Interpretation of holographic interferograms", Optical and Quantum Electronics 8(1976) 469-501

13. M. F. Ashby, "The mechanical properties of cellular solids", Metallurgical Transactions A, 14A (1983)1755-1769.

14. C. Carmichael, Kent's mechanical engineers' handbook , Wiley engineering handbook series, 12th edition, (1950).

15. E. O. Franklin, D. Jones, and H. L. Horton, Machinery's hand book , Industrial Press Inc., 23rd edition, (1988).

16. R. D. Mindlin, "Microstructure in linear elasticity", Arch. Rational Mech. Anal. 16 , (1964) 51-78

17. A. C. Eringen, "Mechanics of micromorphic continua", IUTAM symposium, Mechanics of Generalized Continua, E. Kröner, ed., Springer Verlag, 1968

18. J. L. Bleustein, "Effects of microstructure on the stress concentration at a spherical cavity", Int. J. Solids Structures 2, (1960) 83-104

19. R. S. Lakes, "Deformation mechanisms in negative Poisson's ratio materials: structural aspects", J. Materials Sci. , to appear.

Acknowledgment

Support of this research by the NSF, by the ONR, and by a University Faculty Scholar Award to RSL is gratefully acknowledged. Partial support by the NASA/Boeing ATCAS program under contract #NAS1-18889 is also gratefully acknowledged.

List of figures

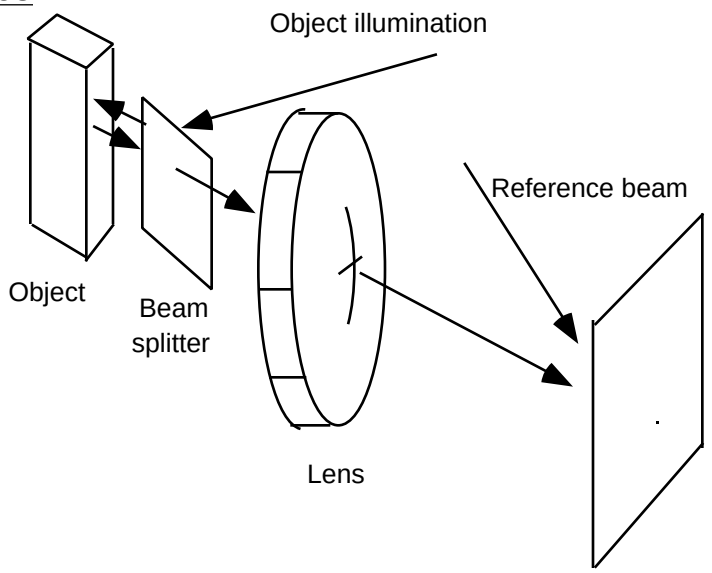

1. Configuration for image plane holography with collimated illumination along the optic axis.

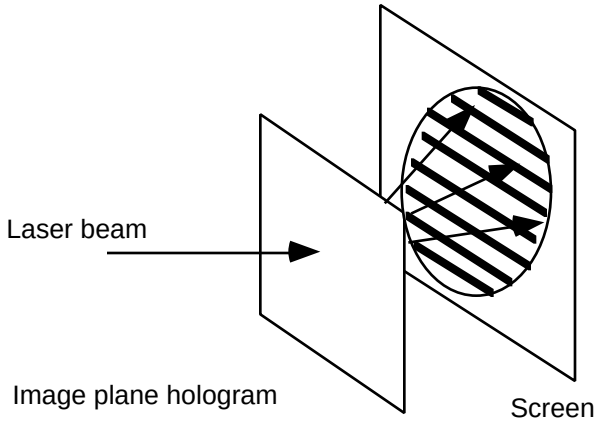

2. Projection of fringes from an image point in the Haidinger fringe method.
3. Fringe pattern of PMMA (Polymethyl Methacrylate) by holographic interferometry, bending test.
4. Fringe pattern of conventional copper foam in bending by holographic interferometry, density 0.795 g/cm^3 with solid volume fraction 0.089.

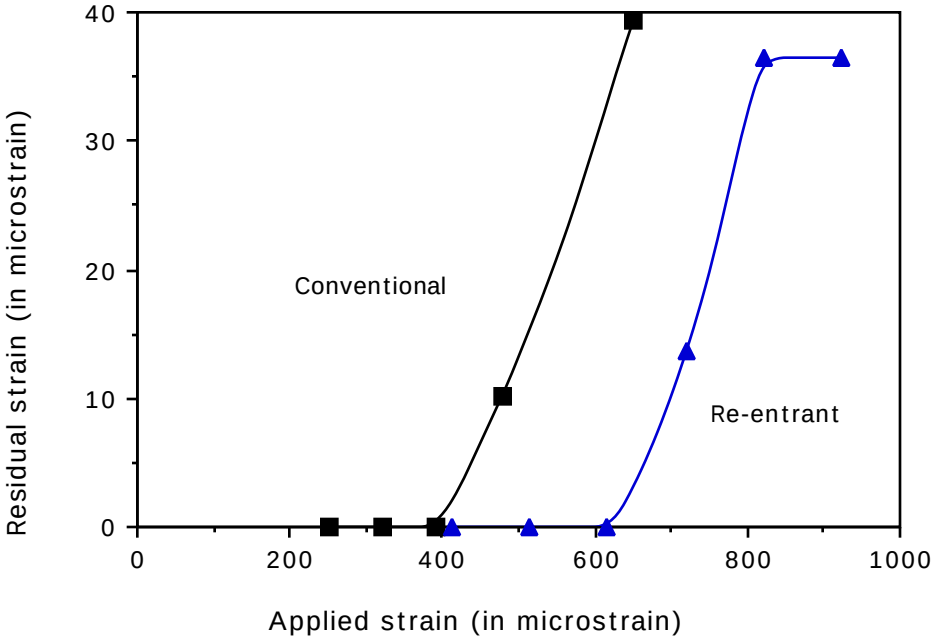

5. Yielding of conventional and re-entrant foam in bending. Residual strain vs applied strain, both in units of microstrain, ie., 10^{-6} strain.

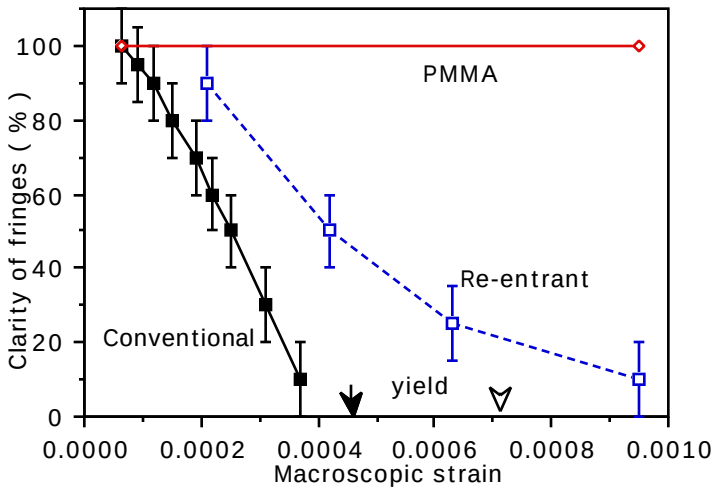

6. The clarity of the fringe pattern vs the macroscopic strain ε, bending test.
Solid square with solid line: conventional copper foam, the downward solid arrowhead denotes the yield point. Open square with dashed line: re-entrant copper foam. ◊: PMMA.
The downward open arrowhead denotes the yield point.

7. Fringe pattern of negative Poisson's ratio copper foam in bending by holographic interferometry, density 2.43 g/cm^3 with solid volume fraction 0.27.